The Influence of Branching Isomerization on the Product Distribution Obtained during Cracking of *n*-Heptane on Acidic Zeolites

A. CORMA,*,1 J. PLANELLES,† AND F. TOMÁS†

*Instituto de Catálisis y Petroleoquímica, CSIC, Serrano 119, Madrid-6, Spain; and †Departamento de Química-Física, Universidad de Valencia, Avenida Dr. Moliner s/n, Burjasot (Valencia), Spain

The initial selectivities for the primary products occurring during the cracking of *n*-heptane on a rare-earth (RE)-HY ultrastable zeolite up to 470°C have been calculated. The activation energies for the cracking of *n*-heptane and its branched isomers in the fraction $C_4 + C_3$ have been obtained by molecular orbital calculations, and these values and the predicted product distribution have been compared with those obtained experimentally. It is concluded that the cracking of *n*-heptane on large-pore zeolites may take place by different parallel routes involving protolytic and β-cracking of *n*-heptane and β-cracking of the readily formed branched carbenium ions. The relative importance of these three routes depends on the Brønsted/Lewis acid site ratio, acid strength distribution, and geometrical factors of the cracking catalyst. © 1985 Academic Press, Inc.

INTRODUCTION

Most of the papers dealing with catalytic cracking of paraffins show that the paraffin/olefin ratio in the products is higher than the value predicted by a classical β-scission mechanism. In a previous work we have reported that for low levels of conversion this behavior could be explained if the reaction takes place on both Brønsted and Lewis sites via protolytic and carbenium cracking, respectively (*1*). However, it is difficult to go deeper into the mechanism of the cracking reactions, mainly because of the impossibility of comparing different works reported in the literature which have been carried out on different catalysts under different experimental conditions, and also because only in a very few reports is a detailed product distribution at initial conditions (low level of conversion and short time on stream) given. Nevertheless, in the case of paraffin cracking on zeolites a high proportion of isobutane (i-C_4) is found in the reaction products (*2–4*). Some authors

(*5, 6*) have suggested that this can be due to the fact that *n*-paraffins can give two parallel reactions, cracking and isomerization, while the branched paraffin obtained by isomerization may also crack in a consecutive step. In this line, Weitkamp et al. (*7–10*) have carried out an extensive study on the hydrocracking of alkanes on PtHY zeolites.

In the present work a detailed product distribution for the cracking of *n*-heptane on a rare-earth (RE)-HY ultrastable zeolite has been carried out. The activation energies for the cracking of *n*-heptane and its branched isomers have been calculated by molecular orbital methods, and the predicted product distribution has been compared with the distribution obtained experimentally.

EXPERIMENTAL

Materials. The catalyst was prepared by repeating three cycles of exchange and calcination of a NaY (Linde SK 40) zeolite with a solution of La^{3+} and Ce^{3+} ions (1/1 atomic ratio) until 85% of the original Na^+ contained in the zeolite had been ex-

---

1 To whom correspondence should be addressed.

changed. The sample was then further exchanged with a NH_4^+ solution, filtered and calcined until 99% of the sodium had been exchanged. After this, the zeolite was pelletized, crushed, and steamed at 530°C for 3 h.

Procedure. The experiments have been carried out in a fixed-bed, tubular reactor heated by an electrical furnace divided into three heating zones. The reactant is charged at the top of the reactor by means of a constant rate positive displacement pump. Thermal effects during the reaction have been minimized by diluting the catalyst with ground glass of the same mesh size up to a constant volume. Condensed liquid products from the reaction are trapped in a pot, after passing through a condenser located below the reactor, while the gaseous products are trapped by the downward displacement of water, saturated with NaCl, in gas burettes.

In a typical run, the reactor is initially purged with N_2 during 20 min at 500°C and then cooled at reaction temperature in the presence of N_2. The flow of N_2 is stopped and 10.0 g of *n*-heptane are pumped through the reactor at a constant rate over a given weight of catalyst (given cat./oil ratio (P)), for a total time t_f. Additional data are obtained at a constant P value by changing the pumping rate. The cat./oil ratio is changed by changing the weight of catalyst. At the end of each run, the reactor is purged with N_2 and all liquid and gaseous products are analyzed. The amount of coke on the catalyst has been obtained measuring the CO_2 and H_2O formed by combustion of the coke with air at 500°C and after passing the combustion gases through a furnace containing CuO pellets.

THEORETICAL CALCULATIONS

The theoretical calculation of the activation energy for a given reaction requires a knowledge of the potential energy hypersurface for the studied reaction system. The calculation of such a hypersurface is not feasible in practice (*11*) for molecules with a number of atoms greater than 3. Consequently, two alternatives to such a calculation are currently used. The first one consists of the calculation of a reduced potential hypersurface by removing some degrees of freedom, which implies an important restriction. The other approximation follows the reaction coordinate method which arbitrarily chooses one degree of freedom X_1 and builds the energy function $\varepsilon(X_1, X_i (\text{min}); i = 2, \ldots, 3N - 6)$ where $X_i(\text{min})$ denotes the other degrees of freedom that have been relaxed to give the minimum value of ε for each X_1. This second alternative is followed in this work.

Scharfenberg (*12*) shows that a minimum of ε corresponds to a minimum on the whole hypersurface E, whereas a maximum of ε corresponds to a saddle point on the hypersurface, that is to the transition state.

It must be kept in mind that the choice of X_1 must be made carefully in order to avoid erroneous results. An inadequate choice can give a chemical hysteresis phenomenon, and also it can happen that the reported maximum will be a "hilltop" instead of a true saddle point if the minimization condition is reduced only to a zero gradient. Nevertheless, in these cases a true saddle point with a slightly modified geometry occurs near the hilltop (*13*). However, this problem does not appear in simple reacting systems such as the β-scission where the reaction coordinate is well defined and a unique, well-defined maximum appears. In spite of this simplification, many calculations must be made in order to outline the hypersurface. Owing to the size of the molecular systems studied the semiempirical MINDO/3 (*14*) method has been used. The use of this simplified method enables us to expand the calculation to many geometrical conformations, and also this method has proved to be a very useful tool for studying the energy and fragmentation reactions of organic ions (*15*).

The applicability of the MINDO/3 method to chemical reactivity studies can be derived from the extensive work of

Bingham *et al.* (*16*) which indicates that the estimated transition state energies are calculated with the same error as those corresponding to equilibrium states; also MINDO/3 calculations for a wide range of systems give an appropriate ordering of the energies of alternative transition states (*17*). Finally, by means of their own adequate parametrization, MINDO/3 calculations take into account correlation effects (*18*) to be considered in the estimation of molecular energies. This circumstance makes MINDO/3 more suitable than many monodeterminantal "ab initio" methods for studying hydrocarbon potential energy hypersurfaces.

The geometry optimization has been performed with a modification of the metric variable method of Murtagh and Sargent (*19*) as realized by Rinaldi (*20*) and applicable to semiempirical methods where the energy can be expanded in mono- and diatomic terms.

Following the above-mentioned methodology, we have proceeded at first to the optimization of the branched heptyl cations (see Table 7 later in the text). From these optimized geometries the β-scission profiles have been outlined. The breaking bond has been taken as the independent variable and all of the internal parameters have been optimized for each value of the independent variable, thus describing the reaction path. The optimization has been performed by maintaining the coplanarity between the breaking bond and the empty p_zAO of the carbenium carbon in order to keep a maximum overlapping during the cracking process as Brouwer and Hogeveen (*21*) suggest. From these profiles we have derived the theoretical activation energies.

RESULTS

In a series of preliminary runs, it was established that in the experimental conditions used in this work thermal cracking is negligible, and no control by external or intraparticle diffusion (particle size 0.5–0.75 mm) was observed. Twenty cycles (re-

action – stripping – regeneration – reaction) were carried out with a sample of the catalyst in order to check its stability and to know the number of experiments which can be safely carried out with a catalyst charge. From the first to the second cycle a slight decrease in *n*-heptane conversion was observed, but after this the conversion remained the same during the 18 additional cycles.

The product yields at constant catalyst-to-oil ratio were plotted versus the experimental cumulative average conversion ($\overline{X}$) for the reaction temperature of 400°C (Fig. 1). In these plots the continuous lines are the Optimum Performance Envelopes (OPE's) (*22*), i.e., the selectivity curves in the absence of deactivation. From these curves one can deduce which products are primary, secondary, stable, or unstable, and also calculate the initial selectivities for the primary products. The initial selectivities for primary products at the three reaction temperatures of 400, 430, and 470°C are given in Table 1. A kinetic procedure described previously (*23*) has been used here to calculate the kinetic and decay parameters, and the resultant values are given in Table 2. By using the kinetic rate constants from Table 2 and the initial selectivities given in Table 3 the kinetic rate constants for the different cracking reactions illustrated in Fig. 2 were also calculated (Table 5) and from their variation with the temperature the corresponding activation energies were obtained (Table 6). The activation energies for the cracking of the different *n*-heptane isomers calculated theoretically are given in Table 7. We have not considered here the processes which give primary carbenium ions, for which the activation energies are of the order of 50 kcal · mol^{-1} (*24*).

DISCUSSION

From the data presented in Table 1, high initial selectivities to i-butane are observed at all three reaction temperatures. In a classical cracking scheme, the *n*-heptane forms
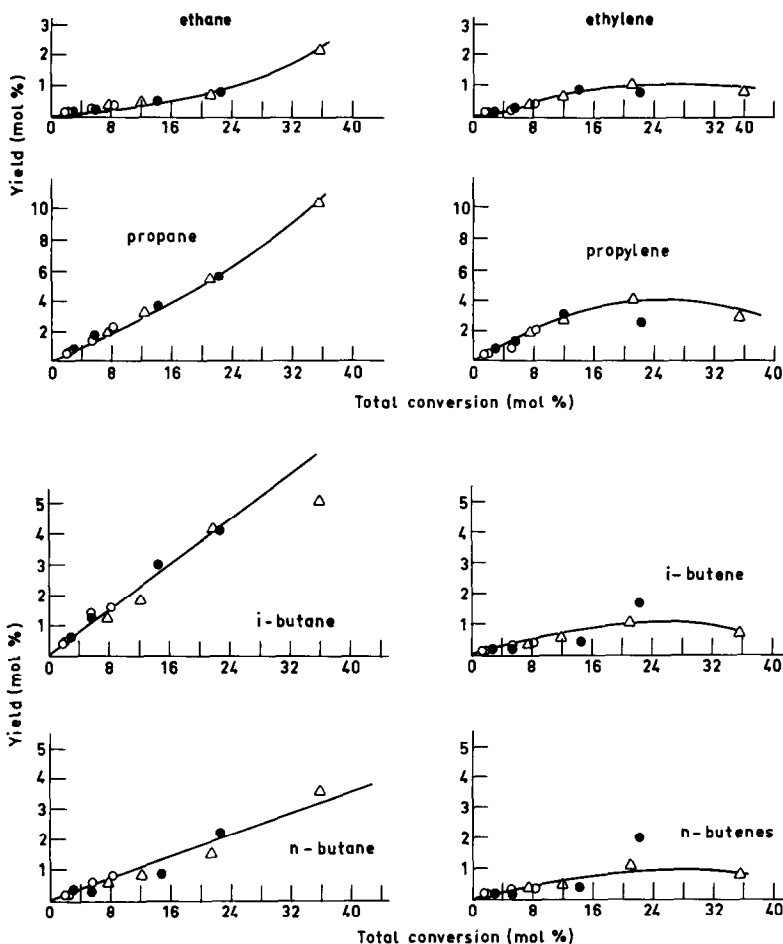
FIG. 1. Selectivity plots for the different reaction products in the cracking of n-heptane on a REHY ultrastable zeolite at 400°C. Continuous lines are the optimum performance envelopes (OPE). Cat./oil: (○) 0.07; (●) 0.146; (△) 0.29.

a carbenium ion which, by β-scission, yields an α-olefin and a primary carbenium ion. The latter gives a secondary carbenium ion by a hydrogen 1,2-shift and can desorb, releasing a paraffin into the gas stream (25, 26).

It is evident that such a mechanism cannot explain the product distribution presented in Table 1, in particular the high initial selectivity for i-butane. Indeed, by a direct cracking of n-heptane through the mechanism described above, the observed products in the C_4 fraction would be n-butane (n-C_4) and n-butenes (n-C_4^{2-}), but not i-butane (i-C_4) and i-butene (i-C_4^{2-}). In order

to explain the high initial selectivity to i-butane one could imagine that the adsorbed n-C_4^+ might give, by a branching rearrangement before desorbing, the i-C_4^+ carbenium ion. This possibility must, however, be rejected in view of the work of Brouwer and Hogeveen (27), who have shown that there is a low rate of isomerization of C_4 paraffin in conditions in which longer-chain paraffins isomerize rapidly. These authors, by working with n-butane labeled with a ^{13}C atom, have observed an extensive scrambling of the ^{13}C atom along the n-butane molecule, but only traces of i-butane. However, in the same experimental conditions,
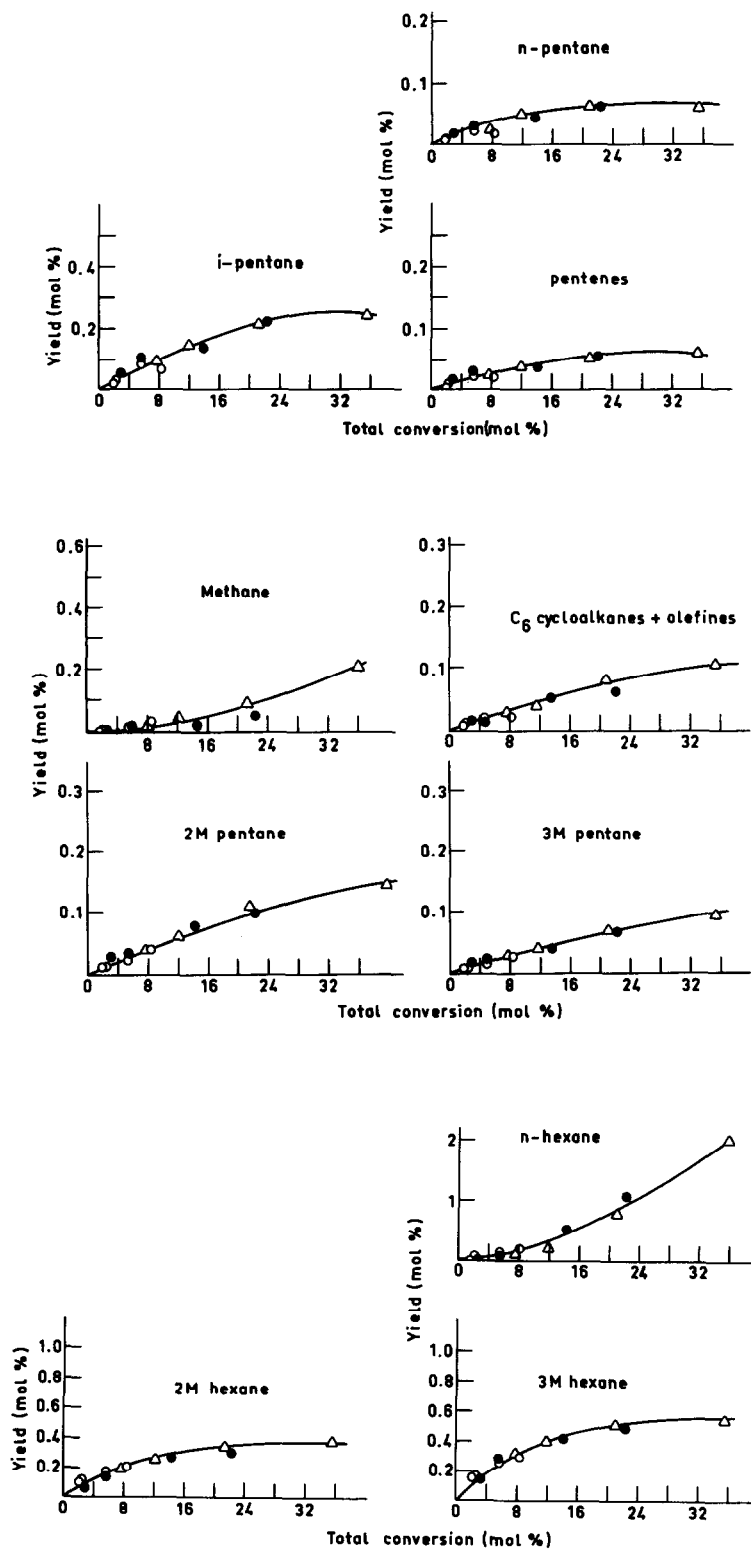
FIG. 1—*Continued*

TABLE 1

Initial Selectivities to the Primary Products During Cracking of n-Heptane on a REHY Ultrastable Zeolite

Product	Reaction temperature (°C)		
	400	430	470
Ethane	0.015	0.015	0.033
Ethylene	0.025	0.015	0.049
Propane	0.21	0.23	0.22
Propylene	0.26	0.24	0.22
i-Butane	0.25	0.22	0.19
n-Butane	0.09	0.08	0.09
i-Butene	0.05	0.07	0.08
n-Butene	0.05	0.06	0.07
i-Pentane	0.020	0.015	0.020
n-Pentane	0.007	0.006	0.012
Pentenes	0.005	0.004	0.008
2M-Pentane	0.006	0.006	0.006
3M-Pentane	0.004	0.005	0.005
n-Hexane + hexenes + cyclohexenes	0.004	0.004	0.005
2M-Hexane	0.032	0.023	0.020
3M-Hexane	0.055	0.035	0.031

n-C_5 or longer n-alkanes can readily isomerize. These results have been explained by Brouwer and Hogeveen by considering that the branching rearrangements go through a protonated cyclopropane intermediate. This mechanism can explain the low isomerization of n-butane to i-butane since such a process implies the formation of primary carbenium ions. If i-butane cannot be

TABLE 2

Fitting Parameters for the Cracking of n-Heptane on a REHY Ultrastable Zeolite

Parameters[a]	Reaction temperature (°C)		
	400	430	470
k (mol/g cat. sec)	153.33	292.48	743.65
G (min^{-1})	80.05	349.04	677.15
N	0.81	0.79	0.79
k_{md} (min^{-1})	64.84	275.74	534.95
m	2.23	2.26	2.26

[a] k, Kinetic rate constant; k_{md}, decay constant; m, order of decay; $G = (m - 1)k_{md}$; $N = 1/m - 1$.

TABLE 3

Initial Selectivities for the Different Cracking Reactions

Reaction[a]	Temperature (°C)		
	400	430	470
1	0.11	0.09	0.07
3	0.25	0.22	0.19
7	0.05	0.07	0.08
2 + 4 + 6	0.05	0.06	0.07
2 + 5	0.015	0.02	0.03

[a] See Fig. 2.

formed by the isomerization of n-C_4^+, it could be generated by cracking of the previously isomerized heptane molecules. On the other hand, since i-butane appears as a primary product, if the cracking of branched isomers is responsible for its formation, the branching isomerization must be much faster than cracking. In other words, the carbocations of the different branched isomers of n-heptane must be in equilibrium on the catalyst surface. Indeed, the 2- and 3-methyl hexane which we could analyze are in equilibrium (Table 1), and therefore we can safely assume that all C_7 isomers are in equilibrium. In the case of the cracked products, the composition of C_5 and C_6 isomers is close to equilibrium, indicating that branching isomerization in C_5^+ and C_6^+ can occur before the carbocation has desorbed. Of course, n- and i-butane are not in equilibrium, in agreement with the work of Brouwer and Hogeveen (27). Thus, some of the C_7 equilibrated carbocations can crack before desorbing, and therefore the final product distribution is going to be strongly influenced by the relative cracking rate of the different n-heptane isomers.

By molecular orbital calculations we have obtained the MINDO/3 activation energies for the β-cracking of all the n-heptane isomers into $C_4 + C_3$ products. One sees (Table 7) that the lowest activation energy corresponds to the cracking of 2,2'-dimethylpentane, which gives as products i-butane plus propylene. These results indi-
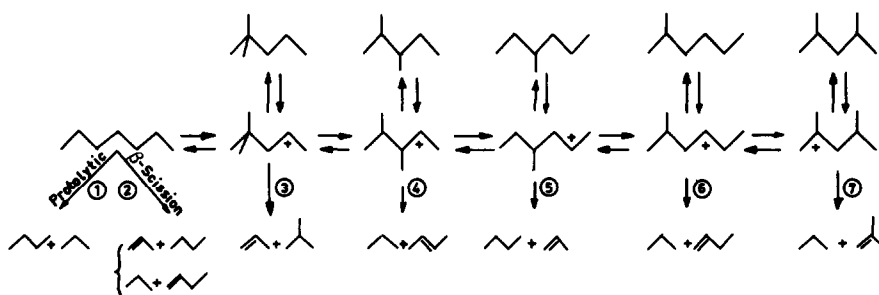
FIG. 2. Cracking reactions of n-heptane and its branched isomers. In the case of branched isomers the reactions giving primary carbenium ions in the products have not been written.

cate that the easiest isomer to be cracked is the 2,2'-dimethylpentane, and consequently the high selectivity for i-butane in the products can be explained via the cracking of the 2,2'-dimethylpentane. This result looks reasonable since such a cracking involves the formation of a tertiary carbenium ion in the product (secondary to tertiary), which is a process preferred to any other involving secondary–secondary or secondary–primary carbenium ions. On the other hand, and if we take into account that the rates of the elementary step of β-scission are given by the product of the intrinsic kinetic rate constant and the concentration of the corresponding surface carbenium ion, the order of rates of cracking of the various heptyl ions, in the range of temperatures studied here, will be given by the order of the apparent kinetic rate constants presented in Table 4. If, as has been found, 2,2'-dimethylpentane is the major source for i-butane, it is clear that by using a zeolite with a pore small enough to

seriously restrict the formation of branched heptanes (28) the initial selectivity to i-butane will decrease. Indeed, we have carried out experiments at 430°C with a H-ZSM-5 zeolite with a Si/Al ratio of 80, and the initial selectivity for i-butane drops from 22% for the REHY zeolite to 6% for H-ZSM-5. This result agrees with those obtained by Jacobs et al. (10, 29) who found that during the hydroisomerization and hydrocracking of paraffins with a Pt/H-ZSM-5 zeolite the formation of dibranched isomers is restricted. If one writes now all the possibilities for cracking C_7 into the fractions $C_4 + C_3$, and taking into account that the protolytic cracking of n-heptane is important during the first moments of Reaction (1) (Fig. 2) until the carbenium surface, i.e., a surface sparsely covered by carbocations, has been formed, one may write for the primary cracking reactions:
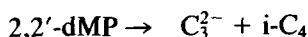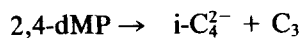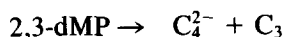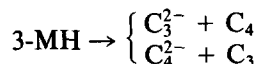
$$n\text{-}C_7H^+ \rightarrow C_{3p} + C_{4p}$$

$$n\text{-}C_7 \rightarrow \begin{cases} C_3^{2-} + C_4 \\ C_4^{2-} + C_3 \end{cases}$$

$$2\text{-MH} \rightarrow \begin{cases} C_4^{2-} + C_3 \\ C_3^{2-} + i\text{-}C_4 \\ i\text{-}C_4^{2-} + C_3 \end{cases}$$

$$3\text{-MH} \rightarrow \begin{cases} C_3^{2-} + C_4 \\ C_4^{2-} + C_3 \end{cases}$$

$$2,3\text{-dMP} \rightarrow C_4^{2-} + C_3$$

$$2,4\text{-dMP} \rightarrow i\text{-}C_4^{2-} + C_3$$

$$2,2'\text{-dMP} \rightarrow C_3^{2-} + i\text{-}C_4$$
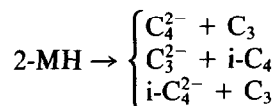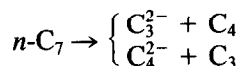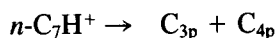
TABLE 4

Initial Selectivities for Propane and n-Butane Obtained via Protolytic Cracking

Temperature (°C)	C_{3p}	C_{4p}
400	0.11	0.08
430	0.10	0.06
470	0.07	0.06

When all these possibilities are taken into account, the following equations can be established

$$C_{3p} = C_{3T} - C_4^{2-} - i\text{-}C_4 \qquad (1)$$

$$C_{4p} = C_{4T} - C_3^{2-} + i\text{-}C_4 \qquad (2)$$

$$C_{3p} = C_{4p}, \qquad (3)$$

where C_{3p} and C_{4p} are propane and n-butane coming from protolytic cracking, C_{3T} and C_{4T} are the total propane and n-butane, respectively, and C_3^{2-}, C_4^{2-}, and i-C_4^{2-} are propylene, n-butenes, and i-butene, respectively. By substituting the corresponding values from Table 1 in Eqs. (1) and (2), one obtains the values given in Table 4.

We have seen above how the initial selectivities (IS) for the products coming from Reaction 1 in Fig. 2 can be calculated. By looking at the rest of the cracking reactions given in Fig. 2, it may be seen that i-butane comes from Reaction 3 and i-butene from Reaction 7. Furthermore, the n-C_4^{2-} is formed through Reactions 2, 4, and 6, and consequently its initial selectivity is directly related to the selectivity for cracking via Reactions (2 + 4 + 6). The initial cracking selectivity for these three reactions can also be calculated from the amount of propane formed.

$$IS[C_3(2 + 4 + 6)] = IS[C_{3T}] - IS[i\text{-}C_4^{2-}] - IS[C_{3p}]$$

Finally, the initial selectivity for the propylene generated by Reactions 2 and 5 is given by the following equation

$$IS[C_3^{2-} (2 + 5)] = IS[C_{3T}^{2-}] - IS[i\text{-}C_4].$$

In Table 3, the calculated initial selectivities for Reactions 1, 3, 7, 2 + 4 + 6, and 2 + 5 are given at the three reaction temperatures.

The kinetic rate constants for 1, 3, 7, 2 + 4 + 6, and 2 + 5 cracking reactions have been calculated taking into account that

$$IS_i = k_i/k.$$

The values of k_i have been obtained (Table 5), and by using the Arrhenius equation the

TABLE 5

Kinetic Rate Constants for the Different Cracking Reactions of n-Heptane on a REHY Ultrastable Zeolite (mol/g cat. sec)

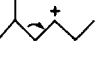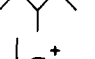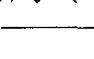| Reactions[a]	Temperature (°C)		
	400	430	470
1	16.87	26.32	52.06
3	38.33	64.35	142.12
7	7.67	20.47	59.49
2 + 4 + 6	7.67	20.47	52.05
2 + 5	2.30	6.82	22.30

[a] See Fig. 2.
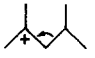
activation energies for the different cracking reactions were calculated (Table 6). One sees that while the activation energy for global cracking of n-heptane into C_3 + C_4 is 23 kcal/mol, two groups of reactions in the different cracking processes appear, one with lower activation energies ($\sim$18 kcal/mol) and the other with higher activation energies ($\sim$30 kcal/mol). The reactions with lower activation energies are the protolytic cracking of n-heptane and the β-scission of 2,2'-dimethylpentane, while those with higher activation energies are the β-cracking of n-heptane, 2- and 3-methylhexane, and 2,3- and 2,4-dimethylpentane. These results are in fairly good agreement with the theoretical activation energies predicted by the molecular orbital calculations (Table 7).

If the cracking reactions can be separated

TABLE 6

Activation Energies for the Different Cracking Reactions of n-Heptane on a REHY Ultrastable Zeolite

Reaction	E_a (kcal/mol)
1	16.1 ± 1.8
3	18.8 ± 2.1
7	29.2 ± 1.2
2 + 4 + 6	27.3 ± 2.8
2 + 5	32.4 ± 1.3
Global	22.6 ± 1.2

TABLE 7

MINDO/3 Activation Energies for β-scission

Reactant	Product	E_a (kcal/mol)
(structure)	$C_3 + i\text{-}C_4^{2-}$	38.3
(structure)	$C_3 + C_4^{2-}$	33.5
(structure)	$C_4 + C_3^{2-}$	30.3
(structure)	$C_3 + C_4^{2-}$	25.5
(structure)	$i\text{-}C_4 + C_3^{2-}$	16.8

in the way presented above it is obvious that the activation energy calculated for the global cracking is not going to be necessarily the same for all acid catalysts. Indeed, the global value is going to depend on factors such as the ratio of Brønsted to Lewis acid sites, acid strength distribution, and shape selectivity of the catalyst. Thus, from a fundamental point of view, the α-test (2), which considers that the activation energy for the global cracking of alkanes is independent of the nature of the acid catalysts, should be questioned. However, in practice, due to the predominance of some of the above reactions, the numerical differences obtained with various catalysts are not very large and consequently the α-test may be used in a first approximation. On the other hand, if cracking data are treated in the way presented in this paper they can give additional information, when comparing cracking catalysts, about the active sites involved in cracking, and the relative amount of those sites on the different cracking catalysts, and on the relation of the acid site composition to the activity, selectivity, and decay characteristics of the catalysts. Hopefully, this information could be used in a following step to tailor cracking catalysts.

In conclusion, we have established that the cracking of n-heptane on a large-pore zeolite may take place by different routes, namely protolytic and β-cracking of n-heptane, and β-cracking of the carbenium ions of the branched isomers. Both Brønsted and Lewis acid sites are active for cracking but through different routes. Finally, the activity, selectivity, and the global activation energy observed on a particular acid catalyst is going to be dependent on factors such the amount of acid sites, the Brønsted/Lewis ratio, the acid strength distribution and geometrical factors on the catalyst.

REFERENCES

1. Corma, A., Planelles, J., Sánchez, J., and Tomas, F., 92, 284 (1985).
2. Miale, J. N., Chen, N. Y., and Weisz, P. B., J. Catal. 6, 278 (1966).
3. Daage, M., and Fajula, F., J. Catal. 81, 394 (1983).
4. Agudo, A. L., Asensio, A., and Corma, A., J. Catal. 69, 274 (1981).
5. Pickert, P. E., Rabo, J. A., Dempsey, E., and Schomaker, V., "Proceedings, 3rd International Congress on Catalysis, Amsterdam, 1964," Vol. II, p. 1264. North-Holland, Amsterdam, 1965.
6. Tung, S. E., and McIninch, E., J. Catal. 10, 166 (1968).
7. Weitkamp, J., Erdoel & Kohle, Erdgas, Petrochem. 31, 13 (1978).
8. Steijns, M., Froment, G., Jacobs, P. A., Uytterhoeven, J. B., and Weitkamp, J., Ind. Eng. Chem. Prod. Res. Dev. 20, 654 (1981).
9. Weitkamp, J., Ind. Eng. Chem. Prod. Res. Dev. 21, 550 (1980).
10. Jacobs, P. A., Martens, J. A., Weitkamp, J., and Beyer, H. K., Faraday Discuss. Chem. Soc. 72, 353 (1982).
11. Müller, K., Angew Chem. Int. Ed. Engl. 19, 1 (1980).
12. Scharfenberg, P., Chem. Phys. Lett. 79, 115 (1981).
13. Dewar, M. J. S., and Kirscher, S., J. Amer. Chem. Soc. 93, 4291 (1971).
14. Bingham, R. C., Dewar, M. J. S., and Lo, D. H., J. Amer. Chem. Soc. 97, 1302, 1311 (1975).
15. Dewar, M. J. S., and Rzepa, H. S., J. Amer. Chem. Soc. 99, 7432 (1977).
16. Bingham, R. C., Dewar, M. J. S., and Lo, D. H., J. Amer. Chem. Soc. 97, 1294 (1975).
17. Flanigan, M. C., Komornick, A., and McIver, J. W., in "Semiempirical Methods of Electron Calculation, Part B: Applications" (G. A. Segal, Ed.), Vol. 8. Plenum, New York, 1977.
18. Bingham, R. C., Dewar, M. J. S., and Lo, D. M., J. Amer. Chem. Soc. 97, 1285 (1975).

19. Murtagh, B. A., Sargent, R. W. H., *Comput. J.* **13,** 185 (1970).
20. Rinaldi, D., *Comput. Chem.* **1,** 109 (1976).
21. Brouwer, D. M., and Hogeveen, H., *Recueil* **89,** 211 (1970).
22. Best, D. A., and Wojciechowski, B. W., *J. Catal.* **44,** 11 (1977).
23. Corma, A., López Agudo, A., Nebot, I., and Tomás, F., *J. Catal.* **77,** 159 (1982).
24. Planelles, J., Sánchez-Marín, J., Tomás, F., and Corma, A., *J. Chem. Soc. Perkin Trans.* **2,** 333 (1985).
25. Haensel, V., "Advances in Catalysis," Vol. 3, p. 179. Academic Press, New York, 1951.
26. Hansford, R. C., "Advances in Catalysis," Vol. 4, p. 1. Academic Press, New York, 1952.
27. Brouwer, D. M., and Hogeveen, H., *Prog. Phys. Prog. Chem.* **9,** 174 (1972).
28. Haag, W. O., Lago, R. M., and Weisz, P. B., *Faraday Discuss. Chem. Soc.* **72,** 317 (1982).
29. Weitkamp, J., Jacobs, P. A., and Martens, J. A., *Appl. Catal.* **8,** 123 (1983).